euronoise

Application of Advanced Features in Computational Acoustics

Reinhard Lerch[a], Manfred Kaltenbacher[a] and Martin Meiler[b]

[a]Univ. Erlangen-Nuremberg, Dept. of Sensor Technology, Paul-Gordan-Str. 3/5, 91052 Erlangen, Germany
[b]Simetris GmbH, Am Weichselgarten 7, 91058 Erlangen, Germany
reinhard.lerch@lse.eei.uni-erlangen.de

Modern numerical simulation tools allow the analysis of the generation and propagation of sound. However, a variety of computational features are missing in these codes. These features are: Frequency dependent damping of the propagation medium, nonmatching grids for computing sound in neighbouring domains with quite different propagation velocities and perfectly matched layers for handling of open domain problems. A finite element environment including pre- and post-processing has been established, and transferred to industry to support the development of electroacoustic devices. The following real life examples will be reported: electrodynamic loudspeakers, noise emission from power transformers, ultrasound devices for medical therapy like lithotripters and a sound protection shield.

1 Introduction

Modern numerical simulation tools allow a precise analysis of acoustic wave phenomena. However, up to now, a variety of computational features enhancing their applicability are missing in these codes. Therefore, it is sometimes cumbersome to come to practically useful results when applying such numerical codes to real life problems. In this paper, some of these lacking features will be addressed in a brief manner. Furthermore, finite element simulations of practical engineering problems will be demonstrated using the recently developed code NACS [1].

When computing the propagation of sound over long distances the numerical errors due to spatial and time **discretization errors** will accumulate. Many sound propagation media exhibit **frequency dependent damping**. When using finite elements in **open domain problems** one has to overcome the difficulty of reflections at the boundaries of the computational domain. When computing sound in neighbouring domains with quite different propagation velocities it is useful to use different finite element grids for these domains, so called **non-matching grids**.

2 Computational Aspects

2.1 Discretization of Wave Phenomena (Dispersion Error)

The application of the classical Galerkin-FEM leads to an increasing numerical error with increasing acoustic wave number $k = \omega / c = 2\pi f / c$ (f and c denotes the frequency and speed of sound). The main effect is due to numerical dispersion, which shows a numerical wave number k^h being different from the continuous wave number k. Therewith, the acoustic waves propagate with a wrong sound speed and show a phase shift compared to the analytical solution. The numerical error e_h due to discretization can be derived as a function of the wave number k and the discretization parameter h [2]

$$e_h \le C_1\theta + C_2 k\theta^2 \text{ with } \theta = kh \qquad (1)$$

C_1, C_2 denote constants which are independent of θ. The first term describes the discretization error, which can be effectively controlled by using accordingly smaller mesh sizes h by increasing wave number k. However, the second term in (1) denotes the *pollution-error*, which increases with k^3 and which leads to severe problems for large wave numbers. In [3] a general formula for this error including the order of the finite element shape functions (p-FEM) can be found, that this part of the error can just be effectively controlled by increasing order of the finite element shape functions.

2.2 Frequency Dependent Damping

The damping of acoustic waves along their propagation paths is an important issue which has to be addressed within precise computer simulations of acoustic phenomena. Damping in the megahertz range for biological matter, for example, suggest the description with a frequency dependency according to a power law. With the two material parameters α_0 and y we can make the following ansatz for the damping coefficient α

$$\alpha(\omega) = \alpha_0 \,|\, \omega \,|^y, \quad 0 < y \le 2\,. \qquad (2)$$

The power factor is a material characteristics and an accurate determination is one of the goals of according measurements [4]. We incorporated attenuation with a power law frequency dependency and dispersion calculated from Kramers-Kronig relations. Both can be combined to a single term in the time domain wave equation [5], which was implemented for transient simulations using a fractional derivative.

2.3 Open Domain Problems (Perfectly Matched Layers)

One of the great challenges for volume discretization schemes is the precise modeling of free radiation problems. The crucial point for these computations is, that the numerical scheme avoids any reflections at the computational boundaries. To achieve this requirement, we have developed an enhanced PML (Perfectly Matched Layer) method, which allows computational domains being a fraction of the acoustic wavelength.

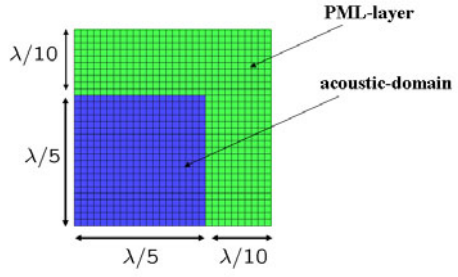

Figure 1: Setup of computational domain

We have evaluated the PML-method, by performing a computation of a 2D example, as displayed in Fig. 1. This example, where we apply an acoustic load at the center, has an analytic solution according to the Hankel function. The total L_2-error as well as the relative error at the corner of the propagation region has been below 0.25 % in any case.

2.4 Matching of Different Grids (Non-Matching Grids)

In this section, we face a common problem within computational acoustics, namely that the computational grid in one subdomain can be considerably coarser than in another subdomain. In order to keep as much flexibility as possible, we use independently generated grids which are well suited for approximating the solution of decoupled local subproblems in each subdomain. Therefore, we have to deal with the situation of nonconforming grids appearing at the common interface of two subdomains. Special care has to be taken in order to define and implement the appropriate discrete coupling operators which are published with more detail in [6]. Here, we will briefly deal with the interface condition of the acoustic-acoustic interface. Therefore, in the strong setting, it is natural to impose continuity in the trace and flux of the acoustic pressure, along the common interface. In our new framework, the flux coupling condition will be enforced in a strong sense by introducing a Lagrange multiplier whereas the continuity in the trace will be understood in a weak sense.

3 Practical Examples

3.1 Electrical Power Transformer

Within the last years the emission of sound has become a very important topic for power transformer manufacturers. Since the customers prescribe a maximum limit of the sound pressure level (SPL) it is very important to gain knowledge about the probable maximum SPL. Therefore, the finite element method is used to compute the sound emission of power transformers. Starting from the winding vibrations of the coils, since these are the reason for the vibrating tank surface, the sound emission will be calculated beginning at the interface between the tank surface and the surrounding air. To obtain free field conditions the above mentioned PML method is used to reduce the computational effort.

Figure 2: Mesh of the Tank

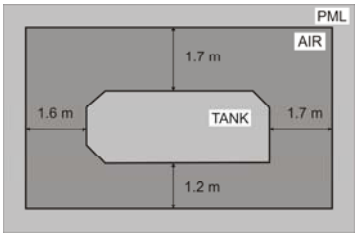

Figure 3: Setup of computational domain

Figure 2 illustrates the meshed model of a transformer-tank. The setup of the computational domain is shown in Fig. 3. The distance between the tank surface and the boundary between the air and the PML region is chosen as in a previously performed measurement.

In the following the SPL computed within the simulation and the measured values will be compared.

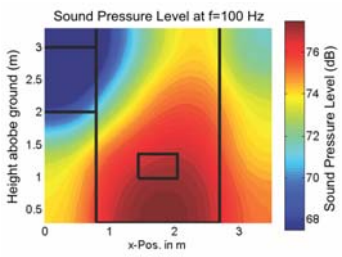

Figure 4: SPL Measured Result

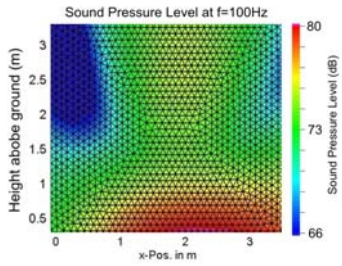

Figure 5: SPL Simulated Result

Figure 4 shows the measured result of the SPL at the main emitting frequency of 100 Hz measured at the left interface between the regions denoted by AIR and PML (see Figure 4). An adequate view of the simulated SPL is shown in Fig. 5. The comparison between both figures shows that the simulation has mainly acquired the distribution of the SPL at the given result surface.

3.2 Electrodynamic Loudspeaker

The electrodynamic loudspeaker to be investigated is shown in Fig. 6. A cylindrical, small, light voice coil is suspended freely in a strong radial magnetic field, generated by a permanent magnet. The magnet assembly, consisting of pole plate and magnet pot, helps to concentrate most of the magnetic flux within the magnet structure and, therefore, into the narrow radial air gap. When the coil is loaded by an electric voltage, the interaction between the magnetic field of the permanent magnet and the current in the voice coil results in an axial Lorentz force. The voice coil is wound onto a former, which is attached to the rigid, light cone diaphragm in order

to couple the forces more effectively to the air and, hence, to permit acoustic power to be radiated from the assembly.

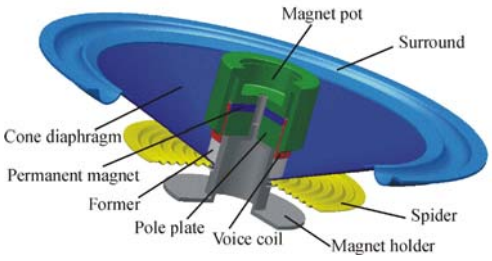

Figure 6: Schematic of an electrodynamic cone loudspeaker

The finite element discretization of the electrodynamic loudspeaker is shown in Fig. 7. Here, the voice coil is discretized by so-called magnetomechanical coil elements based on the *motional emf-term method*, which solves the equations governing the electromagnetic and mechanical field quantities and takes account of the full coupling between these fields. Due to the concentration of the magnetic flux within the magnet assembly, the magnet structure and only a small ambient region have to be discretized by magnetic finite elements. Furthermore, the surround, the spider, the diaphragm and, the former are modeled by mechanical finite elements. Finally, the surrounding fluid region in front of the loudspeaker is discretized by acoustic finite elements. The input level of these simulations is 1 W referred to 4 Ω.

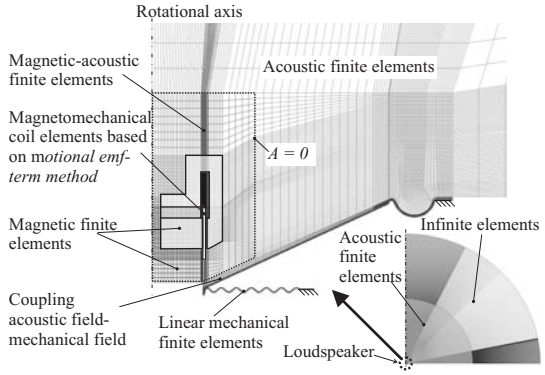

Figure 7: Finite element model of an electrodynamic loudspeaker

The numerical computations concentrate on the two most important design data: the frequency dependencies of the electrical input impedance and the axial sound pressure level. As can be seen in Fig. 8, good agreement between simulation results and measured data was achieved.

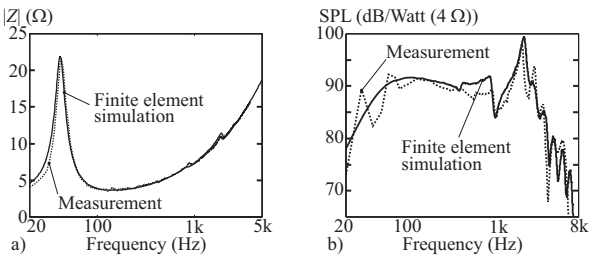

Figure 8: Comparison of simulated and measured results: **(a)** Frequency dependency of electrical input impedance *Z*, **(b)** Axial sound response level SPL at 1 m distance

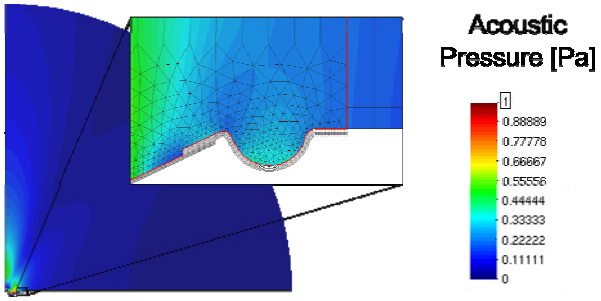

Figure 9: Acoustic pressure amplitude for a frequency of 5 kHz as computed by a nonmatching grid method

In Fig. 9 the results for a harmonic simulation using nonmatching grids is shown. The detail demonstrates the interfaces between the nonmatching parts in the vicinity of the loudspeaker's surround. For the finite element modeling of electrodynamic loudspeakers the utilization of nonmatching grids greatly increases flexibility of pre-processing, especially the meshing process. This allows the use of quite different local discretizations in each subdomain (finer grid for membrane and coarse grid for acoustic field in air). Here, not only the geometry of adjacent elements may be independent but also their order of polynomial approximation is allowed to be different. Therewith, we could use a coarse grid with higher polynomial order for the acoustic field since the solution for the sound field in air is known to be smooth. In contrary, the membrane is modeled by a fine grid consisting of elements with lower order approximation.

Computer-optimization

In the course of this computer-optimization, the knowledge of the sensitivity studies explained in the previous section was put into a new prototype to reduce the even and odd order harmonics under large-signal conditions. As can be seen in Fig.10, significant smaller distortion factors were achieved. In particular, cubic distortion factors could be reduced tremendously. For example, at a frequency of 20 Hz the improvement is 70 % in respect to the original loudspeaker. This significant reduction of cubic harmonics is in accordance with studies concerning the subjective perception of low-frequency distortions [7]. According to [7], odd order harmonics are above all responsible for the deterioration of the sound quality. Furthermore, the important ancillary condition of a similar small-signal behavior in respect to the original loudspeaker must be fulfilled. Small-signal simulations resulted in an acceptable reduction in efficiency of -0.5 dB.

Furthermore, the numerically predicted improvements in the large-signal behavior of the loudspeaker could be successfully confirmed by measurements on the new prototype (see Fig. 10). Therefore, it can be stated that the developed simulation scheme is well suited to the industrial computer-aided design of electrodynamic loudspeakers, since an optimization with a significant reduced number of prototypes can be achieved.

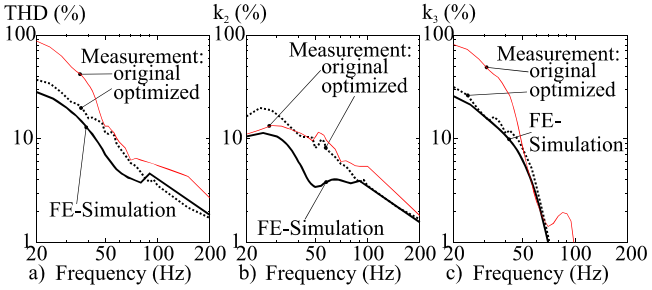

Figure 10: Comparison of simulated and measured distortion factors of the optimized loudspeaker (at an input power of 16 W): a) Total Harmonic Distortion (THD, b) Quadratic distortion factor k_2, c) Cubic distortion factor k_3

3.3 High-Power Pulse Sources for Lithotripsy

The acoustic power source for lithotripsy is based on an electromagnetic principle, and its schematic setup is displayed in Fig. 11.

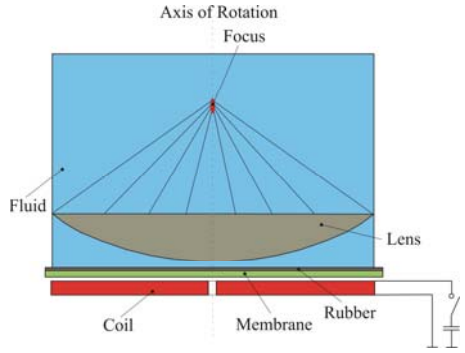

Figure 11: Schematic of an electromagnetic driven acoustic power source

When the slab coil is loaded by a capacitor discharge, eddy currents are induced in the metallic membrane. The interaction between these eddy currents and the overall magnetic field results in a magnetic volume force (Lorentz force) acting on the membrane. Therewith, the membrane-rubber structure is deformed and an acoustic pulse is radiated into the fluid and focused by the lens. For the numerical simulation a finite element grid width of 90 µm (corresponds to about 70 finite elements per fundamental wavelength) was used for the acoustic domain. Since in this case, we have to consider the non-linearities within the electromagnetic transducer, we perform the numerical simulation in two steps:

Transducer Computation

Since the non-linearities of the acoustic field near the transducer can be neglected, we compute the acoustic pressure using the linear acoustic wave equation. Therewith, we fully take into account the fluid loading of the transducer. For modeling the electromagnetic transducer we consider all relevant non-linearities (updated Lagrangian formulation for the magnetic field, geometric non-linearity for the aluminum membrane and the non-linear electromagnetic force term).

3.4 Non-linear Wave Propagation Computation

In a second run, we fully solve Kuznetsov's non-linear wave equation using the computed pressure near the transducer obtained from the first simulation step.

The measured and simulated pressure signals in the focus region of the source are shown in Fig. 12.

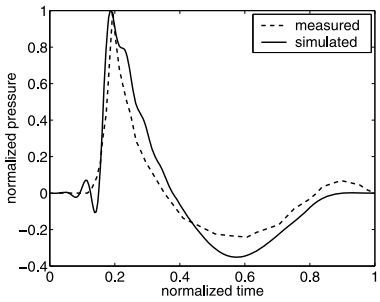

Figure 12: Comparison between measured and simulated sound pressure level in the focal region of the electromagnetic pulse source

3.5 Sound Protection Shield

As a result of increasing car traffic on highways or main roads the neighboring residents are complaining about the heavy traffic noise. Therefore, sound protection shields have to be built to provide a tolerable noise level. The shape of the sound protection shields as well as the material and thickness are parameters that may be varied to obtain an optimum solution. These parameter variations can easily be done by applying the finite element method.

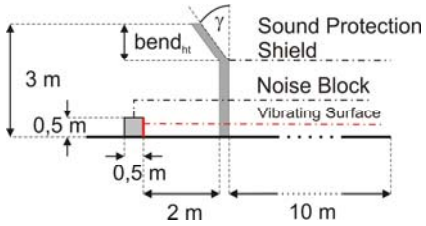

Figure 13: Setup of noise block and sound protection shield

Figure 13 shows the setup of the given system. A noise block with a vibrating surface emits acoustic waves of a fixed frequency f=100 Hz. The sound protection shield is placed 2 meters in front of the noise block. The angle γ as well as the bend height $bend_{ht}$ are parameter that can be varied. To ensure free field conditions a Perfectly Matched Layer method is applied to the boundary of the computational domain.

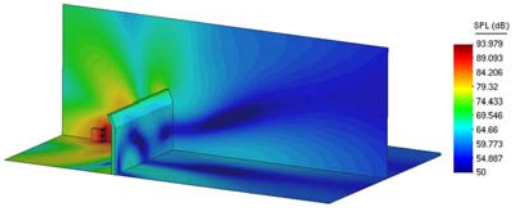

Figure 14a: SPL with bend height 0.5 m

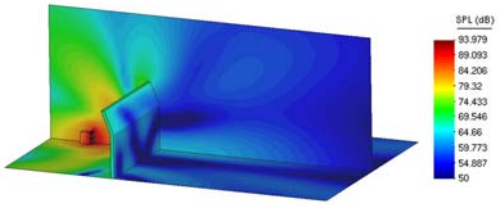

Figure 14b: SPL with bend height 1.0 m

Figure 14a and 14b show the simulation results for two variations of the bend height. Comparing the SPL results it is obvious that an increasing height of the sound protection shield results in decreasing sound pressure levels behind the shield.

4 Conclusions

In this paper we first addressed some problems within computational acoustics when doing finite element calculations. These are frequency dependent discretization errors as well as damping of the propagation medium. Furthermore, we presented two useful tools, which are perfectly matched layers and non-matching grids. When performing calculations in the frequency domain, perfectly matched layers allow the ideal absorption of acoustic energy at the border of the computational domain. Therewith, they are useful for the treatment of open domain problems. Non-matching grids enhance the efficieny and accuracy of finite element calculations which ask for different mesh sizing in different subdomains. In the second part of the paper, practical engineering examples, based on a new finite element code, have been demonstrated.

References

[1] www.simetris.de

[2] F. Ihlenburg, I. Babuska, *SIAM J. Numer. Anal.*, 34:315-358 (1997)

[3] M. Ainsworth, *SIAM J. Numer. Anal.*, 42:553-575 (2004)

[4] L. Bahr, M. Kaltenbacher, R. Lerch, *Proceedings of the IEEE Ultrasonics Symposium*, 1687-1690 (2005)

[5] K. R. Waters, M. S. Hughes, G. H. Brandenburger, J. G. Miller, *J. A. S. A.*, 108(5):2114-2119, November 2000. Pt. 1.

[6] B. Flemisch, M. Kaltenbacher, B. I. Wohlmuth, *Int. J. Numer. Meth. Engng*, 67(13):1791-1810 (2006)

[7] G. Krump, “Concerning the perception of low-frequency distortions”, *Fortschritte der Akustik DAGA 2000*, Oldenburg, 486-488 (2000)